The impact of the North Atlantic Oscillation on the uptake and accumulation of anthropogenic CO_2 by North Atlantic Ocean mode waters

Naomi Marcil Levine,[1,2] Scott C. Doney,[3] Ivan Lima,[3] Rik Wanninkhof,[4] Nicholas R. Bates,[5] and Richard A. Feely[6]

Received 9 June 2010; revised 3 May 2011; accepted 10 June 2011; published 21 September 2011.

[1] The North Atlantic Ocean accounts for about 25% of the global oceanic anthropogenic carbon sink. This basin experiences significant interannual variability primarily driven by the North Atlantic Oscillation (NAO). A suite of biogeochemical model simulations is used to analyze the impact of interannual variability on the uptake and storage of contemporary and anthropogenic carbon (C_{anthro}) in the North Atlantic Ocean. Greater winter mixing during positive NAO years results in increased mode water formation and subsequent increases in subtropical and subpolar C_{anthro} inventories. Our analysis suggests that changes in mode water C_{anthro} inventories are primarily due to changes in water mass volumes driven by variations in water mass transformation rates rather than local air-sea CO_2 exchange. This suggests that a significant portion of anthropogenic carbon found in the ocean interior may be derived from surface waters advected into water formation regions rather than from local gas exchange. Therefore, changes in climate modes, such as the NAO, may alter the residence time of anthropogenic carbon in the ocean by altering the rate of water mass transformation. In addition, interannual variability in C_{anthro} storage increases the difficulty of C_{anthro} detection and attribution through hydrographic observations, which are limited by sparse sampling of subsurface waters in time and space.

Citation: Levine, N. M., S. C. Doney, I. Lima, R. Wanninkhof, N. R. Bates, and R. A. Feely (2011), The impact of the North Atlantic Oscillation on the uptake and accumulation of anthropogenic CO_2 by North Atlantic Ocean mode waters, *Global Biogeochem. Cycles*, *25*, GB3022, doi:10.1029/2010GB003892.

1. Introduction

[2] Since the industrial revolution, human activity has released large quantities of carbon dioxide (CO_2), resulting in increased atmospheric concentrations [e.g., *Keeling et al.*, 1976; *Keeling and Whorf*, 1994; *Le Quéré et al.*, 2009]. However, the observed atmospheric increase accounts for only approximately half of anthropogenic carbon emissions [*Canadell et al.*, 2007; *Le Quéré et al.*, 2009; *Sabine et al.*, 2004] (http://www.globalcarbonproject.org). The remaining anthropogenic CO_2 has been taken up by the oceans and terrestrial biospheres, with approximately 25% of anthropogenic CO_2 emissions currently being sequestered in the oceans [*Le Quéré et al.*, 2009, 2010]. The future trajectory of atmospheric CO_2, and the resulting impact on the global climate, is therefore dependent on the magnitude and stability of the ocean and terrestrial carbon sinks [*Canadell et al.*, 2007; *Friedlingstein et al.*, 2006; *Fung et al.*, 2005; *Le Quéré et al.*, 2009].

[3] Over the past three decades, the oceanographic community has devoted significant time and resources to accurately detect both the accumulation of anthropogenic carbon (C_{anthro}) in the ocean and variability in the ocean carbon sink [*Sabine and Tanhua*, 2010]. This is done through full depth surveys of water column dissolved inorganic carbon (DIC) concentrations and anthropogenic tracers and through measurements of surface-ocean partial pressure of carbon dioxide (pCO_2) and air-sea CO_2 fluxes. Several global surveys of the ocean inorganic carbon system have been conducted including the Geochemical Ocean Section Study (GEOSECS) in the 1970s and the World Ocean Circulation Experiment (WOCE)/Joint Global Ocean Flux Study (JGOFS), and Ocean-Atmosphere Carbon Exchange Study (OACES) surveys in the 1990s [*Key et al.*, 2004; *Lee et al.*, 2003; *Sabine et al.*, 2004]. Currently, the U.S. and International Climate Variability and Predictability (CLIVAR)/CO_2 Repeat Hydrography Program is continuing to monitor changes in ocean DIC by resurveying key hydrographic cruises from

[1]MIT-WHOI Joint Program, Woods Hole, Massachusetts, USA.
[2]Now at Department of Organismic and Evolutionary Biology, Harvard University, Cambridge, Massachusetts, USA.
[3]Marine Chemistry and Geochemistry, Woods Hole Oceanographic Institution, Woods Hole, Massachusetts, USA.
[4]NOAA/AOML, Miami, Florida, USA.
[5]Bermuda Institute of Ocean Sciences, St. George's, Bermuda.
[6]NOAA/PMEL, Seattle, Washington, USA.

Copyright 2011 by the American Geophysical Union.
0886-6236/11/2010GB003892

the WOCE/JGOFS era. In addition, approximately 4.8 million measurements of surface water pCO_2 have been made between 1970 and 2006 and assembled into a uniform data set. These prodigious field efforts have provided data to assess the magnitude and variability of the ocean carbon sink [e.g., *Takahashi et al.*, 2009; *Watson et al.*, 2009]. However, while significant headway has been made, the detection of C_{anthro} in the ocean still faces several major challenges.

[4] The C_{anthro} signal is superimposed upon a large dissolved inorganic carbon (DIC) background, with C_{anthro} accounting for only about 5% of the total reservoir of DIC in surface waters in the 1990s [*Sabine et al.*, 2004]. In addition, significant short-term natural variability in the ocean carbon system makes the detection of relatively small, long-term temporal trends in C_{anthro} difficult [*Levine et al.*, 2008]. Several empirical methods have been proposed to deconvolve the C_{anthro} signal from natural variability in the ocean carbon system [e.g., *Brewer et al.*, 1995; *Friis et al.*, 2005; *Gruber et al.*, 1996; *Khatiwala et al.*, 2009; *Matsumoto and Gruber*, 2005; *Touratier and Goyet*, 2004; *Wallace*, 1995; *Waugh et al.*, 2006]. However, each of these methods has their own biases resulting in significant uncertainties in C_{anthro} estimates, particularly in regions of water mass formation [*Levine et al.*, 2008; *Vázquez-Rodríguez et al.*, 2009]. Finally, hydrographic cruises are expensive and provide limited temporal and spatial resolution.

[5] The synergistic use of observations and numerical models has become an important tool for understanding the ocean carbon sink; observations provide an important check of model output, and model results provide a context for interpreting observations and insight into the mechanisms controlling the uptake and accumulation of C_{anthro} [e.g., *Sarmiento et al.*, 1995]. This study uses the output of a global ocean model to investigate the impact of interannual variability on the uptake and storage of C_{anthro} in the North Atlantic Ocean and to provide a context for observations of C_{anthro} in this basin. Nearly 25% of anthropogenic carbon sequestered in the ocean is found in the North Atlantic Ocean, despite the fact that this basin only accounts for 15% of the global area [*Sabine et al.*, 2004]. Changes in uptake and accumulation of carbon in this region therefore have the potential to significantly impact the global inventory of C_{anthro}. In addition, a mechanistic understanding of North Atlantic Ocean dynamics may provide insight into interannual variability in C_{anthro} storage in other basins. Finally, understanding the underlying mechanisms driving C_{anthro} trends will also help improve models used to project future changes in atmospheric CO_2 and global climate.

[6] Mode waters play an important role in the circulation, heat transport, and biogeochemistry of ocean gyres [e.g., *Marshall et al.*, 2009; *McCartney and Talley*, 1982]. These waters form during the winter and carry water with high C_{anthro} into the ocean interior where residence times range from years to many decades [*Wallace*, 2001]. Here we investigate carbon uptake by subtropical and subpolar mode waters, two key water masses for determining variability in North Atlantic Ocean C_{anthro} sequestration in our model. The primary subtropical mode water in the western North Atlantic Ocean is the Eighteen Degree Water (EDW), which forms southeast of the Gulf Stream during the winter months between 33°N–40°N and 30°W–75°W [e.g., *Talley and Raymer*, 1982]. Variability in EDW formation and CO_2 uptake has been shown to correlate with climate modes such as the North Atlantic Oscillation [*Bates et al.*, 2002; *Bates*, 2007; *Gruber et al.*, 2002; *Joyce et al.*, 2000]. However, the driving mechanisms behind these correlations remain unclear [*Bates*, 2007]. A summary of previous findings in the context of this study is presented in section 6.1.

[7] Mode water formation occurs primarily through water mass transformation (formation through diapycnal mixing and surface buoyancy flux) [e.g., *Brambilla et al.*, 2008] and is therefore strongly influenced by wintertime mixed layer depths (MLD) [e.g., *Brambilla and Talley*, 2008; *Marshall et al.*, 1993; *McCartney and Talley*, 1982]. In the subpolar gyre, dense mode water (SPMW) is formed in the northeastern subpolar gyre and travels counterclockwise around the gyre and into the Labrador Sea where some of it ultimately becomes part of the Labrador Sea Water (LSW), a component of North Atlantic Deep Water [*Brambilla et al.*, 2008; *McCartney and Talley*, 1982; *Talley and McCartney*, 1982]. Understanding the properties and history of the densest SPMW, therefore, provides insight into the properties of LSW [*McCartney and Talley*, 1982], an important sink for C_{anthro}. A number of studies have quantified changes in the subpolar ocean carbon sink based on observations of surface pCO_2 [*Corbière et al.*, 2007; *Lefèvre et al.*, 2004; *Omar and Olsen*, 2006; *Schuster and Watson*, 2007; *Takahashi et al.*, 2009; *Watson et al.*, 2009] and profiles of DIC and anthropogenic tracers [*Friis et al.*, 2005; *Olsen et al.*, 2006; *Pérez et al.*, 2008, 2010; *Steinfeldt et al.*, 2009]. The observed temporal rates of change of air-sea CO_2 flux and C_{anthro} inventories, which range in different analyses and for different regions from an increase in the North Atlantic Ocean carbon sink to a decrease in the basin sink, are highly dependent on the time period of the observations. *Thomas et al.* [2008], *Schuster et al.* [2009] and *Watson et al.* [2009] suggest that these differences may be due to limited observational records which alias interannual variability, such as the North Atlantic Oscillation, into estimates of long-term trends.

[8] The North Atlantic Oscillation (NAO) is the major climate mode driving interannual and decadal variability in the North Atlantic Ocean [*Hurrell*, 1995]. During positive NAO years, the combination of a strong atmospheric low pressure over Iceland and a strong atmospheric high pressure in the tropics results in increased storm frequency and current strength in the North Atlantic, Labrador and Nordic Seas [e.g., *Hurrell et al.*, 2003, 2001; *Visbeck et al.*, 2003]. During a negative NAO, the Icelandic atmospheric low pressure system shifts southward resulting in more southerly storm tracks, fewer storms, and weaker currents in the North Atlantic Ocean [e.g., *Hurrell et al.*, 2001]. The shift from a negative to positive NAO has been shown to correlate with a northward migration of the Gulf Stream [*Hurrell and Deser*, 2009; *Marshall et al.*, 2001]. While there is insufficient data to determine the impact of the NAO on MLD in the subpolar and northern subtropical gyres, positive NAO years correlate with decreased sea surface temperatures (SST) in this region indicating that MLD may increase during positive NAO years as there is a negative relationship between SST and MLD [*Hurrell and Deser*, 2009]. The strength of the NAO (the NAO index) is typically measured during the winter months, December–March [*Rogers*, 1984]. The past four decades have seen significant interannual variability in

the NAO index, with the most prominent feature being an extended period of positive NAO from 1988 to 1995. For this study we use the station-based wintertime NAO record for 1970–2004 compiled by James Hurrell (National Center for Atmospheric Research, Boulder CO USA, http://jisao.washington.edu/data_sets/nao/).

[9] Several recent modeling studies have looked at the impact of the NAO on the North Atlantic Ocean carbon sink [*McKinley et al.*, 2004; *Thomas et al.*, 2008; *Ullman et al.*, 2009; *Watson et al.*, 2009]. These studies have focused on interannual changes in air-sea CO_2 flux, surface pCO_2, and upper ocean (100 m) DIC. *Thomas et al.* [2008] propose that changes in the NAO have resulted in significant interannual variability in the subpolar and basin-scale air-sea CO_2 flux. In contrast, *McKinley et al.* [2004] find no significant relationship between air-sea CO_2 flux and the NAO index, which they attribute to long air-sea equilibrium timescales for the carbonate system resulting in a slow response in surface pCO_2. Using the same model as *McKinley et al.* [2004], *Ullman et al.* [2009] find a strong relationship between the first principal component of the subpolar air-sea CO_2 flux and the NAO index and a significantly weaker correlation between pCO_2 and the NAO index. These authors suggest that surface variability in pCO_2 and DIC is driven by changes in vertical transport in the subpolar gyre and by fluctuations in temperature in the subtropical gyre. However, the implication of these surface changes on the thermocline inventory of anthropogenic carbon in the North Atlantic Ocean and the underlying mechanisms driving these changes remains unclear.

[10] Here we use a suite of model simulations to deconvolve the mechanisms driving interannual variability in the North Atlantic Ocean C_{anthro} inventory in the subpolar and subtropical gyres. The NAO plays a significant role in modulating the formation of mode waters and the accumulation of anthropogenic carbon in model simulations. Specifically, shifts from a negative to positive NAO phase result in deeper mixing in mode water formation regions in both gyres. This in turn increases the modeled anthropogenic CO_2 air-sea flux and rates of water mass transformation, thereby increasing C_{anthro} inventories along mode water isopycnals. The impact of NAO shifts on mode water C_{anthro} inventories has important implications for the future of the North Atlantic Ocean carbon sink as climate models predict an increased frequency of positive NAO years [*Meehl et al.*, 2007].

2. Methods

2.1. Model Description

[11] The ocean Biogeochemical Element Cycle (BEC) component of the National Center for Atmospheric Research (NCAR) global Community Climate System Model (CCSM-3) is used for this study [*Doney et al.*, 2009a, 2009b]. The model is noneddy resolving with a grid spacing of 3.6° longitude by 0.8°–1.8° latitude and 25 vertical levels. Mesoscale eddies are parameterized according to *Gent and McWilliams* [1990]. The model contains a full ecological module [*Moore et al.*, 2004] with several phytoplankton function groups and multinutrient limitation including iron limitation. The fourteen main compartments of the ecological module are: small/pico phytoplankton, large phytoplankton/diatoms, nitrogen fixing diazotrophs, zooplankton, suspended and sinking detritus, nitrate, ammonia, phosphate, iron, silicate, oxygen, DIC and alkalinity. The biogeochemistry module [*Doney et al.*, 2006, 2009a] includes full carbonate system thermodynamics, CO_2 air-sea gas exchange, a dynamic iron cycle, and dust deposition from an atmospheric transport model. Neither photosynthesis nor calcification is dependent on CO_2 variables. A full description of the BEC model, including the spin-up and initialization procedure, can be found in the work of *Doney et al.* [2009a, 2009b]. Briefly, the model was spun-up for several hundred years to a quasi-equilibrium state using preindustrial CO_2 (280 ppm) and a repeating annual cycle of atmospheric state variables [*Large and Yeager*, 2004]. The 'repeat annual cycle' is constructed based on a typical year from the hindcast period and maintains realistic high frequency forcings (e.g., storms) consistent with the climatological record.

[12] For this study, we use four companion model simulations that were branched in a consistent fashion from the end point of the spin-up simulation:

[13] 1. Preindustrial CO_2 Repeat Annual Cycle (RAC): The model is forced with the 'repeat annual cycle' used for the long-term spin-up. Atmospheric CO_2 is fixed at preindustrial levels (280 ppm).

[14] 2. Transient CO_2 Repeat Annual Cycle: The model is branched from the quasi-equilibrium steady state in 1870 and run through 2004 forced with the 'repeat annual cycle' and atmospheric CO_2 prescribed following ice core measurements and observations (Pieter Tans, NOAA/ESRL (http://www.esrl.noaa.gov/gmd/ccgg/trends/, download date 2010).

[15] 3. Preindustrial CO_2 Variable Physics (VP): The model is branched from the Preindustrial CO_2 Repeat Annual Cycle in 1958 and run for a historical hindcast simulation from 1958 to 2004 forced with atmospheric reanalysis and satellite data products [*Doney et al.*, 2007, 2009a]. Atmospheric CO_2 is fixed at preindustrial levels (280 ppm).

[16] 4. Transient CO_2 Variable Physics: The model is branched from the Transient CO_2 Repeat Annual Cycle in 1958 and run with the same forcing as Preindustrial CO_2 Variable Physics but with atmospheric CO_2 prescribed following observations (Pieter Tans, NOAA/ESRL (http://www.esrl.noaa.gov/gmd/ccgg/trends/, download date 2010).

[17] For this study we focus on the period of 1970–2004 as these years show the greatest interannual variability in C_{anthro} inventory and have available historical field observations.

2.2. Calculations

[18] Contemporary carbon ($C_{contemp}$) is defined as the DIC concentration for model simulations with increasing atmospheric CO_2. Anthropogenic carbon in the model is determined by subtracting the DIC concentration for paired model simulations with identical physics but with varying and constant atmospheric CO_2:

$$C_{anthro} = C_{contemp} - C_{preindustrial} \quad (1)$$

where $C_{preindustrial}$ is the DIC concentration for the simulation with constant preindustrial atmospheric CO_2 concentrations. The impact of variable ocean physics is investigated by differencing C_{anthro} for the 'Repeat Annual Cycle' (RAC)

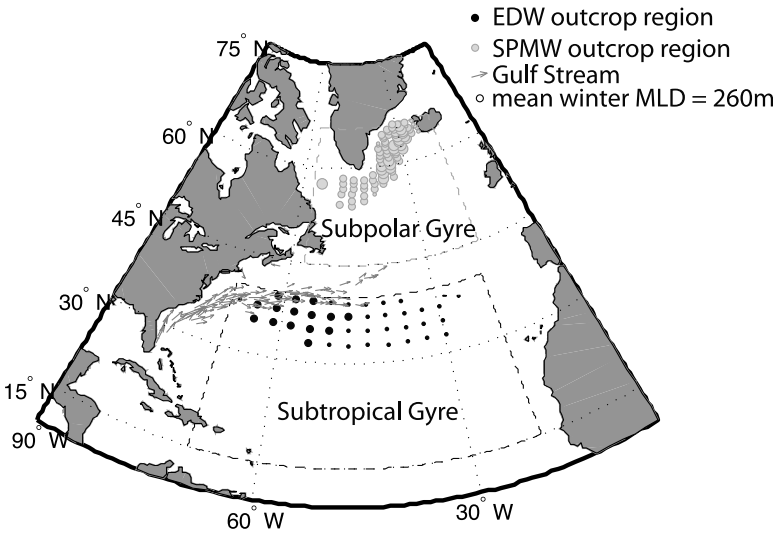

Figure 1. Map of study region. The boundaries used for the subtropical (black dashed line) and subpolar (gray dashed line) are demarcated. The model wintertime outcrop region for the subtropical mode water (Eighteen Degree Water, EDW) and Subpolar Mode Water (SPMW) are shown using black and gray circles, respectively. The size of the circle corresponds to the average wintertime mixed layer depth (MLD). The average wintertime location of the Gulf Stream is shown using dark gray arrows (data from *Mariano et al.* [1995]).

model simulation from the 'Variable Physics' (VP) model simulation:

$$\chi_y^{\Delta physics} = \chi_y^{VP} - \chi_y^{RAC} \tag{2}$$

where $\chi_y^{\Delta physics}$ is the impact of variable physics on either carbon concentrations ($C_{contemp}^{\Delta physics}$, $C_{anthro}^{\Delta physics}$) or carbon inventory ($I_{contemp}^{\Delta physics}$, $I_{anthro}^{\Delta physics}$), and χ_y^{VP} and χ_y^{RAC} are carbon concentrations or inventories calculated using equation (1) for the 'Variable Physics' and 'Repeat Annual Cycle' model simulations, respectively. $C_{contemp}$ and C_{anthro} are given in μmol kg^{-1}. Column inventories ($I_{contemp}$, I_{anthro}) are calculated as the sum of $C_{contemp}$ or C_{anthro} either over a fixed depth or over isopycnal surfaces (isopycnal band) and expressed in mol C m^{-2}. Unless otherwise specified, carbon inventories are calculated for the model mixed layer and thermocline (0–1280 m to be precise based on the model vertical grid). Latitude areal inventories are the areal integral of column inventories falling within a latitude range and are expressed in Tg C (10^{12} g C). Changes in carbon inventory with time are calculated as:

$$\Delta I_y^{\Delta physics} = \left. \left(I_y^{\Delta physics}(Dec_{t1}) - I_y^{\Delta physics}(Dec_{t0}) \right) \right/ 1year \tag{3}$$

where $\Delta I_y^{\Delta physics}$ is the change in $I_{contemp}$ or I_{anthro} over one year defined as December to November. This interval was chosen instead of the conventional January–December interval to allow for better comparison with the NAO winter index, which is calculated for December–March. For example, $\Delta I_y^{\Delta physics}$ for December 1970 to November 1971 is compared to the NAO winter index for December 1970 to March 1971.

[19] To evaluate the impact of interannual variability on anthropogenic carbon storage in subtropical mode waters (hereafter called "Eighteen Degree Water," EDW), we focus on the wintertime EDW formation region and the $26.25 \leq \sigma_\theta \leq 26.75$ ($\sigma_{26.25–26.75}$) isopycnal band. *Bates et al.* [2002] use a potential density of 26.4 kg m^{-3} for the EDW surface, however, in the model the EDW surface is closer to 26.5 kg m^{-3}. The EDW formation region is defined as the region where the mean surface temperature (upper 50 m) falls between 17.8° and 18.4°C during the winter months (January–March) [after *Bates et al.*, 2002]. The location of the model EDW formation region for the VP model simulations is shown in Figure 1. The wintertime anthropogenic CO_2 flux into the EDW formation region is calculated as the total net anthropogenic CO_2 flux into the model ocean during January–March and is expressed in Tg C a^{-1}. The subtropical areal integral of I_{anthro} for $\sigma_{26.25–26.75}$ is calculated as the sum of the column inventories by area across the $\sigma_{26.25–26.75}$ band between 15°N–40°N and 20°W–70°W where $\sigma_{26.25–26.75}$ is deeper than 150 m (Figure 1). Integrating over the entire gyre area effectively removes the influence of isopycnal heave (vertical shifts), and minimizes the impact of water mass sloshing (horizontal shifts) on changes in I_{anthro} as horizontal shifts in water mass boundaries will result in similar shifts in isopycnal surfaces.

[20] Our analysis of interannual variability in anthropogenic carbon storage in the subpolar gyre focuses on the Subpolar Mode Water (SPMW). For this study, we identify seven SPMW density classes. We focus our analysis on the densest SPMW in the eastern basin, σ_θ values between 27.55 and 27.7, as these waters have a longer residence time than lighter SPMW and are the precursor to LSW [*Brambilla and Talley*, 2008]. The subpolar I_{anthro} for the SPMW isopycnal surfaces are calculated as the areal integral of the column inventories across the individual SPMW isopycnal bands for the area between 45°N–66°N and 57°W–18°W, which corresponds to the SPMW formation regions in the central and eastern subpolar gyre (Figure 1). The winter outcrop region for the

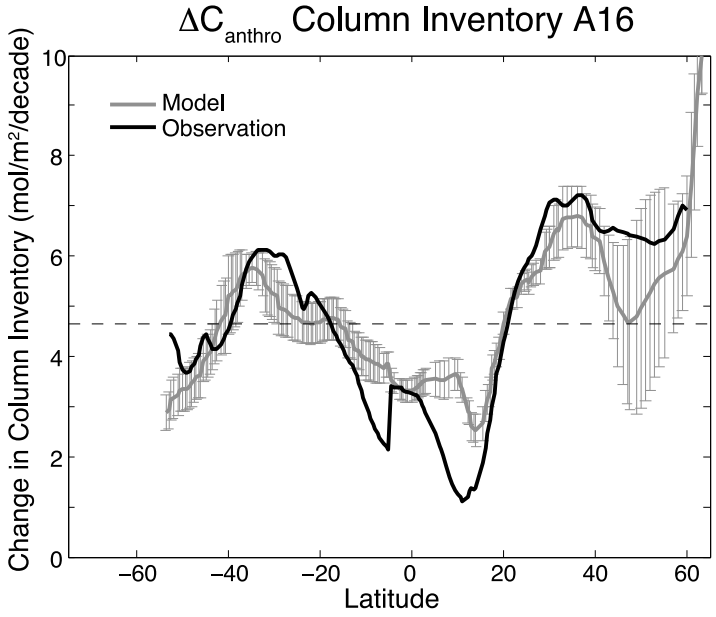

Figure 2. Comparison between model and observational estimates [*Wanninkhof et al.*, 2010] of the rate of change of C_{anthro} column inventory (upper 1280 m) along the Atlantic Ocean north-south A16 transect. Model error bars represent the natural variability in the model system and are calculated according to equation (4). The observational error (not shown) is approximately 10% [*Wanninkhof et al.*, 2010].

densest SPMW is defined as the region where the $\sigma_{27.6–27.7}$ isopycnal band outcrops during the winter months (January–March). The location of the model SPMW formation region for the VP model simulation is shown in Figure 1. Since this work focuses on the North Atlantic Ocean, we limit our analysis to south of 70°N. The wintertime uptake of anthropogenic CO_2 by the $\sigma_{27.6–27.7}$ SPMW is calculated as the sum of the net anthropogenic CO_2 flux into the $\sigma_{27.6–27.7}$ winter outcrop region expressed in Tg C a^{-1}.

2.3. Model Skill

[21] The physical oceanographic component of the CCSM BEC reproduces observed spatial and temporal trends in sea surface height, temperature, and circulation [*Doney et al.*, 2007]. The spatial pattern and seasonal cycles of model air-sea CO_2 flux and surface pCO_2 agree with global observations with an RMS error at the grid scale of 1.53 mol CO_2 m^{-2} a^{-1} and 18.6 μatm, respectively [*Doney et al.*, 2009b]. The BEC model response to NAO forcing is also consistent with observed changes in circulation, vertical mixing, salinity and surface temperature [*Thomas et al.*, 2008].

[22] To evaluate model skill at reproducing I_{anthro}, the model output was extracted for the CLIVAR/CO_2 north-south Atlantic Ocean hydrographic section (A16) for the year and months of the A16 occupations: February 1989 and December 2004 for the south Atlantic Ocean, and July–August 1993 and June–August 2003 for the north Atlantic Ocean. As the model was only run through December 2004, this month was used for the second occupation of A16 south instead of the actual occupation dates, January–February 2005. Model I_{anthro} for the A16 section was calculated following equation (1) and integrating over the upper 1280 m. The decadal change in model I_{anthro} in mol m^{-2} $decade^{-1}$ is compared to the observed C_{anthro} inventory for 0 m – 1280 m [*Wanninkhof et al.*, 2010] in Figure 2. Along the A16 transect, this depth range accounts for 81% of model C_{anthro} and 93% of observed C_{anthro}. For each station along the A16 transect, the decadal variability in model I_{anthro} during the occupation period (1989–2004) is estimated as:

$$\textit{model variability}(stn_x) = \sqrt{\frac{1}{N-1}\sum_{i=1}^{N}\left(\Delta I^{10yr}_{anthro}(stn_x) - \overline{\Delta I^{10yr}_{anthro}(stn_x)}\right)^2} \quad (4)$$

where ΔI^{10yr}_{anthro} is the decadal change in I_{anthro} at station X for each month between January 1989 and December 2004 (i.e., January 1999 minus January 1989, February 1999 minus February 1989, etc.), $\overline{\Delta I^{10yr}_{anthro}(stn_x)}$ is the mean of the monthly decadal changes in I_{anthro} at station X from 1989 to 2004, and N is the number of monthly $\Delta I^{10yr}_{anthro}(stn_x)$ measurements (N = 72, 6 years of monthly data). This variability is shown as error bars in the model estimate in Figure 2. The RMS difference of model I^{model}_{anthro} from the observational I^{obs}_{anthro} is given by:

$$\textit{RMS difference} = \sqrt{\frac{\sum_{x=1}^{N}\left(I^{model}_{anthro} - (I^{obs}_{anthro}\right)^2}{N-1}} \quad (5)$$

where N is the number of A16 stations (N = 173). The model estimates a mean uptake rate of 4.7 mol m^{-2} $decade^{-1}$ and compares favorably with the spatial pattern of C_{anthro} uptake for the Atlantic Ocean section determined from observations with an RMS difference of 0.84 mol m^{-2} $decade^{-1}$. The envelope encompassing the RMS variability of the model estimates overlaps the observational estimate of *Wanninkhof et al.* [2010] over much of the subtropics and subpolar region,

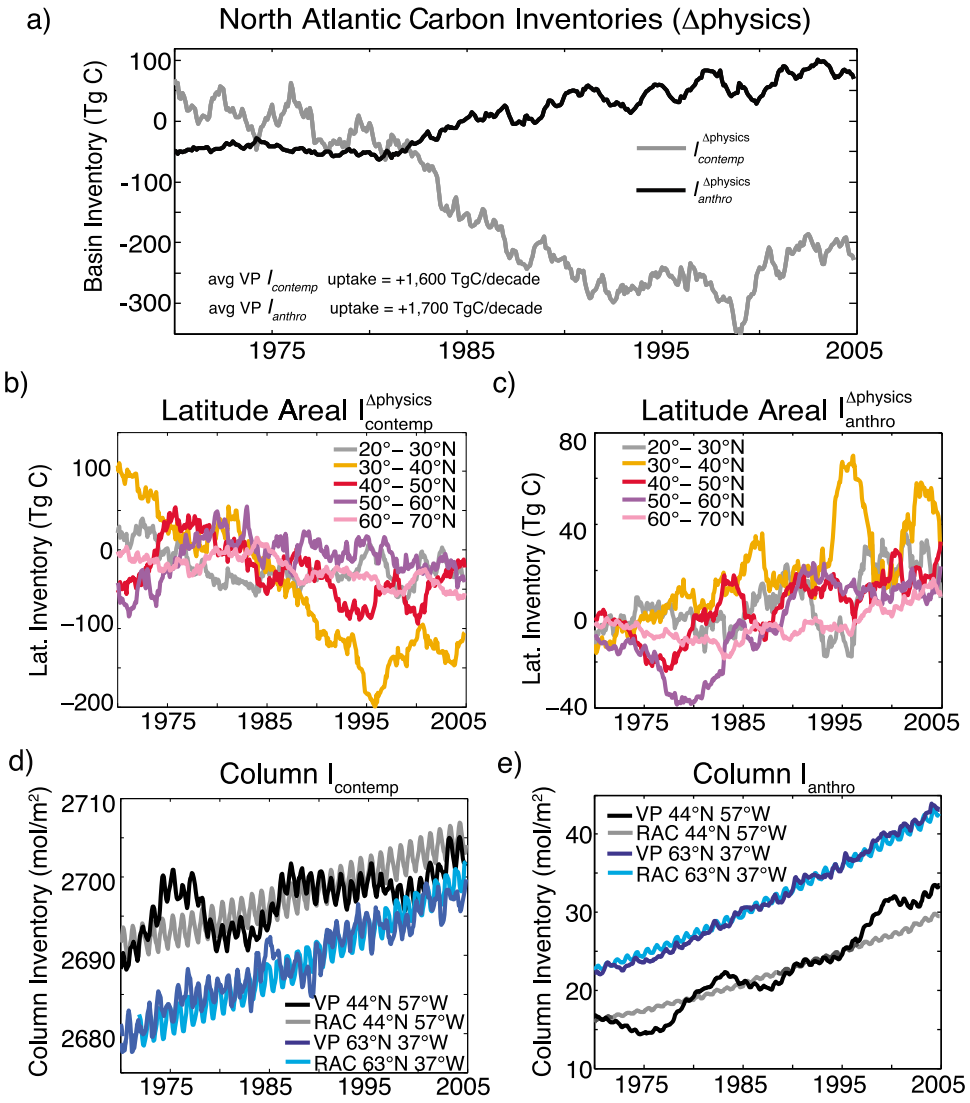

Figure 3. Change in model $I_{contemp}$ and I_{anthro} with time for (a) the North Atlantic Ocean basin, 15°N–70°N, (b and c) latitude areal inventories, and (d and e) column inventories for 44°N 57°W and 63°N 37°W. All inventories are calculated for the upper 1280 m. Figures 3a and 3c plot the Δphysics inventories ($I^{\Delta physics}_{contemp}$ and $I^{\Delta physics}_{anthro}$) where Δphysics is a measure of ocean sensitivity to variable climate and ocean circulation as defined by equation (2). Figures 3d and 3e plot the output for both the VP and RAC model simulations. Figure 3a also gives the mean I_{anthro} uptake rate and the mean increase in $I_{contemp}$ for the North Atlantic Ocean basin in Tg C per decade from 1970 to 2005 for the VP model simulation.

the focus of this study. In addition, the BEC model reproduces most of the observed vertical structure of anthropogenic carbon concentrations, temperature, salinity, DIC, and alkalinity along the A16 transect (Figures S1 and S2).[1] Further analysis, including a full synthesis of C_{anthro} observations, is needed in order to understand the differences between the model and observations in particular at low latitudes.

3. Variability in Ocean Carbon Pools

[23] Variable ocean physics results in seasonal, interannual, and decadal variability in North Atlantic Ocean $I_{contemp}$ and I_{anthro} on local (10s kilometers) and regional to basin (100s kilometers) scales. For both pools, variability is greatest on small spatial scales and is dampened at larger scales. Specifically, variable physics has only a small impact on North Atlantic Ocean carbon inventories when integrated over the entire basin, 15°N–70°N (Figure 3a; monthly coefficient of variation of 0.02% and 0.52% for $I_{contemp}$ and I_{anthro}, respectively), but results in increased $I_{contemp}$ and I_{anthro} variability for integrated latitudinal band inventories (Figures 3b and 3c; monthly coefficient of variation of 0.01–0.06% and 0.56–1.61%, respectively) and at the local scale (Figures 3d and 3e; monthly coefficient of variation of 0.02–0.22% and 0.74–9.41%, respectively). Different scales of variability indicate the importance of water mass sloshing, isopycnal heave, and shifts in gyre boundaries,

[1] Auxiliary materials are available with the HTML. doi:10.1029/2010GB003892.

all of which impart large variations on small scales but do not impact carbon inventories at larger scales. In addition, these results also suggest that changes in ocean forcing (e.g., increased frequency of positive NAO years) may impact the magnitude of regional carbon sinks in the North Atlantic Ocean, for example the storage of C_{anthro} in mode waters, and complicate detection studies. While the scales of variability are similar for $I_{contemp}$ and I_{anthro}, the impact of variable physics is often of opposite sign (e.g., Figure 3). Recent modeling studies show that long-term trends in anthropogenic air-sea CO_2 flux can be inversely related to changes in the natural air-sea CO_2 flux [*Lovenduski et al.*, 2008]. Similarly, our analysis demonstrates that, while changing model physics results in a slight increase in anthropogenic carbon accumulation rate in the North Atlantic Ocean basin between 1970 and 2004, variable model physics causes a decreased accumulation rate of contemporary carbon over this time period (Figure 3a).

[24] Changes in carbon inventories are driven by variations in air-sea CO_2 gas exchange and physical transport as well as, for $I_{contemp}$, variability in biological carbon uptake and export. The inclusion of variable ocean physics results in significant interannual fluctuations in latitudinal areal accumulation rates (dI/dt) in the VP simulation relative to the RAC simulation (Figures 3b and 3c), with variations of up to −81% to +118% for $dI_{contemp}/dt$ and −36% to +38% for dI_{anthro}/dt (calculated as the change over a 5 year interval). This indicates that variable ocean physics may alter the rate at which the ocean sequesters carbon. As suggested above, a substantial portion of changes in latitude areal and local scale $dI_{contemp}/dt$ and dI_{anthro}/dt is due to sloshing and heave. For example, the decrease in dI_{anthro}/dt between 20°N–30°N in the early 1990s and subsequent increase in inventory between 30°N–40°N (Figure 3c) appears to be primarily due to a northward shift in the subtropical gyre boundary resulting from a transition to an extended positive NAO (discussed further below). These substantial changes in column inventories due to shifts in water mass boundaries increase the difficulty of detection and attribution of anthropogenic CO_2 uptake with hydrographic observations, a challenge that may be addressable with models.

[25] To isolate the impact of variable physics on water mass carbon inventories, we analyze the change in $\Delta I^{physics}_{contemp}$ and $\Delta I^{physics}_{anthro}$ for isopycnal bands in the subtropical ($\sigma_{26.25–26.75}$, 14–40°N, 20–70°W) and subpolar ($\sigma_{27.3} - \sigma_{27.7}$, 45°N–66°N, 57°W–18°W) gyres. $\Delta I^{\Delta physics}$ for the subtropical isopycnal band and several subpolar bands appears to be impacted by model bias (differences in the mean state of the VP versus RAC model), with $\sigma_{26.25–26.75}$, $\sigma_{27.55–27.6}$ and $\sigma_{27.65–27.675}$ showing a negative bias and $\sigma_{27.675–27.7}$ showing a positive bias (Figure S4). We assume that this bias results from a difference in mean model state and so all interannual variability (changes in $\Delta I^{\Delta physics}$) is directly attributable to changes in model physics (see auxiliary material, Text S1, section S2, for further discussion of model bias). However, due to the potential for different biases along different SPMW surfaces, it is necessary to evaluate the density bands individually rather than as a cumulative inventory. For this study we focus on the $\sigma_{27.675–27.7}$ isopycnal band, as this band is significantly impacted by variable physics, displays significant interannual variability in anthropogenic carbon accumulation rate, and is one of the densest SPMW in the model simulation and so is likely to be an important precursor to LSW (see Text S1, section S3).

[26] Variable physics induces substantial subannual to decadal variability in the subtropical $\sigma_{26.25–26.75}$ and subpolar $\sigma_{27.675–27.7}$ water mass volumes, anthropogenic and contemporary carbon inventories, and mean anthropogenic and contemporary carbon concentrations (Figure 4 and Table S1). In both gyres, variations in contemporary and anthropogenic inventories along the isopycnal bands are driven by changes in water mass volume (Figures 4a and 4b). For anthropogenic carbon, changes in I_{anthro} are also positively correlated with changes in mean C_{anthro} concentration (r value of 0.55 and 0.64 for the subtropics and subpolar gyres, respectively). This suggests that the physical mechanisms driving changes in water mass volumes may also impact mean C_{anthro} concentrations. In the subpolar gyre, there is an anticorrelation between the mean C_{anthro} and the mean $C_{contemp}$ along the isopycnal band. This is primarily due to the opposing vertical concentration gradients of these two pools (Figures 4f and 5). This decoupling is not observed in the subtropical gyre where there is a weak positive correlation between mean $C_{contemp}$ and mean C_{anthro} ($r = 0.18$, $p < 0.01$). The impact of variable physics on contemporary and natural carbon inventories in the ocean has significant implications for the global carbon cycle and warrants further study. However, here we focus on the mechanisms responsible for the interannual variability in C_{anthro} uptake and storage in the subtropical (section 4) and subpolar (section 5) gyres.

4. Mechanisms Governing Interannual Variability in the Subtropical Gyre

[27] In the BEC model, constant ocean physics results in a stable wintertime (January–March) EDW formation region between 35 and 38°N, whereas the addition of variable ocean physics causes the location of the outcrop region to oscillate between 33°N and 40°N. The northward extent of the EDW formation region determines the area of the outcrop, with a poleward shift in the northern boundary resulting in periods of increased outcrop area. As expected, a larger outcrop footprint results in an increased anthropogenic CO_2 flux into the EDW. Variable ocean physics (VP simulation) also increases MLDs in the EDW formation region; the spatial averaged maximum MLDs increases from 292m ± 1 (1σ) to 337m ± 31 (1σ), resulting in additional increased uptake of anthropogenic CO_2 by the EDW (*not shown*).

[28] As the EDW formation region is located directly south of the Gulf Stream, poleward shifts in the Gulf Stream and subtropical/subpolar boundary will result in a subsequent northward shift in the EDW formation region. Positive NAO years have been shown to result in such a northward shift of the Gulf Stream by approximately 1 degree [*Joyce et al.*, 2000]. In the VP model, a positive NAO year generally results in a similar northward shift in the EDW formation region by a little over 1 degree. There is also a positive relationship between the NAO wintertime index, the mean EDW MLD, and the flux of anthropogenic CO_2 into the EDW formation region (Table 1). In both observational studies [e.g., *Joyce et al.*, 2000] and the BEC model, ocean memory causes the subtropics to respond to NAO atmospheric forcing with a lag of 1–2 years [*Curry and McCartney*, 2001].

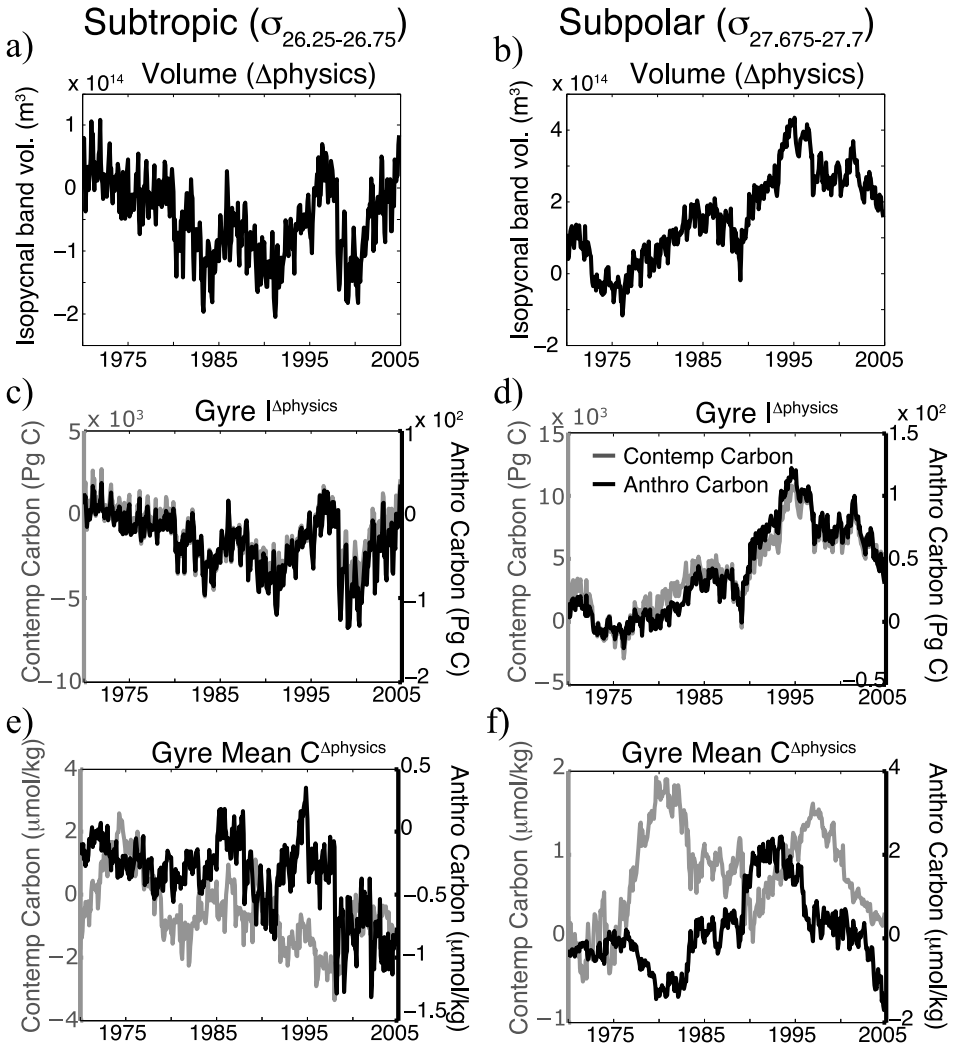

Figure 4. Sensitivity of model isopycnal bands to variable physics for (a, c, and e) the subtropical $\sigma_{26.25–26.75}$ isopycnal surface between 15°N–40°N, 20°W–70°W and >150 m and (b, d, and f) subpolar SPMW isopycnal surface ($\sigma_{27.675–27.7}$) between 45°N–66°N, 57°W–18°W. Figures 4a and 4b present Δphysics volume for the two isopycnal bands. Figures 4c and 4d show the Δphysics inventories for contemporary and anthropogenic carbon ($I^{\Delta physics}_{contemp}$ and $I^{\Delta physics}_{anthro}$), and Figures 4e and 4f show the mean Δphysics contemporary and anthropogenic carbon inventories. Δphysics is defined by equation (2).

Therefore, the values for the subtropics presented in Table 1 are given with a lag of 2 years. These relationships suggest that, during a positive NAO phase, the Gulf Stream moves northward causing a similar shift in the EDW formation region, greater EDW formation rates (thicker EDW isopycnal band) due to increased outcrop area and deeper mixed layer depths, and increased uptake of C_{anthro} onto the EDW surface.

[29] Interannual variability in anthropogenic carbon storage in the subtropical gyre is highly correlated with changes in advective convergence, in particular with the horizontal convergence of carbon (see Text S1, section S4). This is consistent with previous work, which showed that interannual changes in DIC and temperature in the subtropics are dominated by advective transport [*Doney et al.*, 2007, 2009a]. Our analysis suggests that most of the changes in I_{anthro} observed in the gyre interior are due to C_{anthro} anomalies or changes in isopycnal thickness advected from outcrop regions where large scale mixing events and air-sea CO_2 fluxes occur.

[30] Changes in EDW wintertime anthropogenic air-sea CO_2 flux (smoothed with a three year running mean) are positively correlated with changes in $\sigma_{26.25–26.75}$ gyre inventory ($\Delta I^{\Delta physics}_{anthro_{\sigma 26.25–26.75}}$), with a slope of 9.9 ± 4.7 $^{PgI_{anthro}a^{-1}}/_{PgCO_2a^{-1}}$ for the regression of $\Delta I^{\Delta physics}_{anthro_{\sigma 26.25–26.75}}$ on the wintertime air-sea CO_2 flux (r = 0.36, p = 0.04). This indicates that changes in the EDW formation region air-sea CO_2 flux only accounts for approximately 10% of the change in $\Delta I^{\Delta physics}_{anthro_{\sigma 26.25–26.75}}$. Increased EDW I_{anthro} can either be derived from increased local air-sea CO_2 flux or from the transformation of lighter, high C_{anthro}, density classes into the EDW density class. As discussed previously, the air-sea CO_2 flux into the EDW outcrop region is highly correlated with the EDW wintertime footprint and mean MLD in the formation region. Therefore, increased air-sea CO_2 flux will correlate with increased rates of water mass transformation. We believe that the relationship between wintertime CO_2 flux and $\Delta I^{\Delta physics}_{anthro_{\sigma 26.25–26.75}}$ is

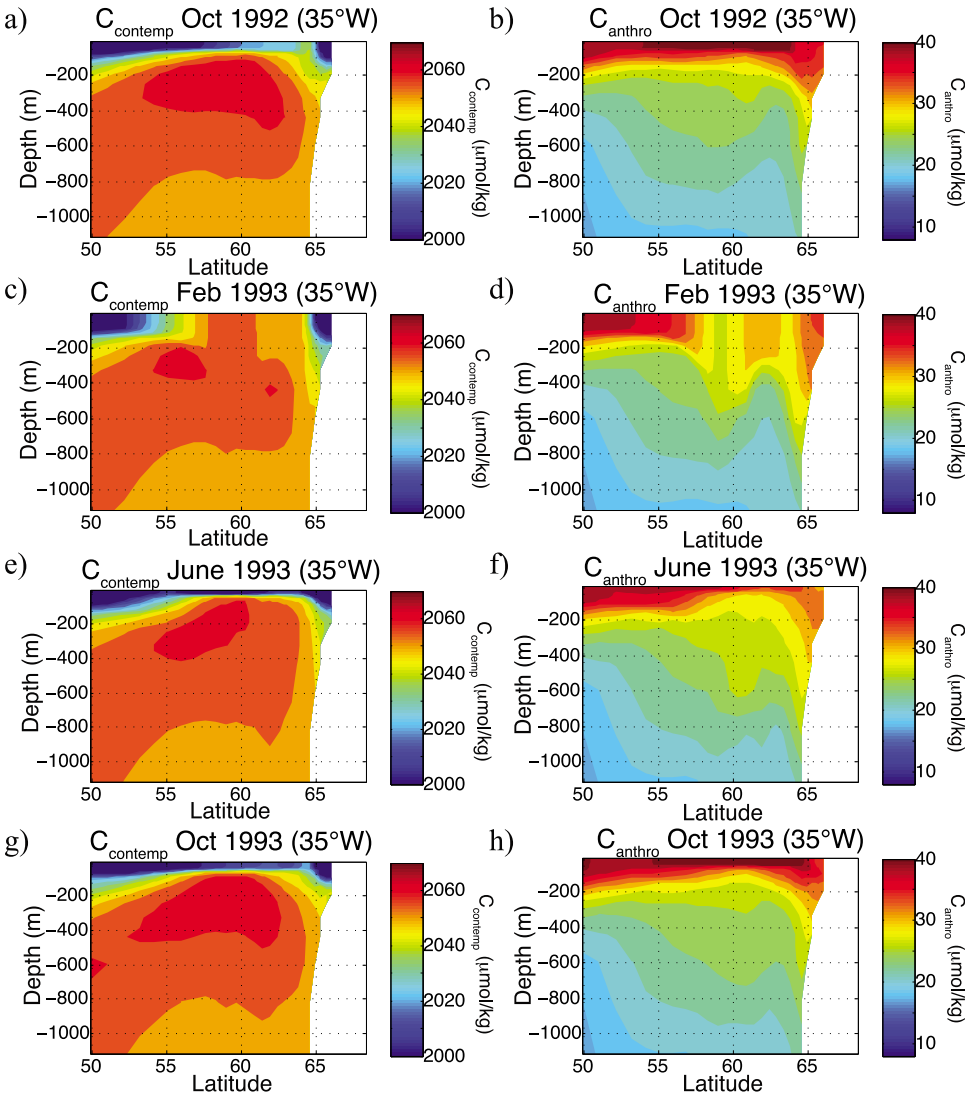

Figure 5. The effect of seasonal convection and restratification in the model subpolar gyre. (a, c, e, and g) Plot of VP $C_{contemp}$ (μmol kg^{-1}) along a north-south transect at 35°W. (b, d, f, and h) Plot of VP C_{anthro} (μmol kg^{-1}) along the same transect. The depth transects for October 1992, and February, June, and October 1993 are plotted in Figures 5a and 5b, 5c and 5d, 5e and 5f, and 5g and 5h, respectively. In October, high C_{anthro} concentrations are observed in the stratified surface waters; Figures 5b and 5h. During the deep winter mixing events, these high C_{anthro} waters are mixed with underlying low C_{anthro} waters resulting in dense, high C_{anthro} mode waters; Figure 5d. In the spring and summer, stratification of the surface waters return but the remnants of high C_{anthro} from the winter mixing is still apparent at depth; Figure 5f. The opposite pattern occurs for $C_{contemp}$ due to the difference in surface to depth concentration gradients between $C_{contemp}$ and C_{anthro}.

a proxy for changes in $\Delta I^{\Delta physics}_{anthro_{\sigma 26.25-26.75}}$ driven by fluctuations in water mass transformation rates. This is consistent with the findings of *Alfultis and Cornillon* [2001], who suggest based on temperature profiles that overlying waters are entrained into the EDW during wintertime mixing events. The relationship between changes in the EDW formation region and shifts in the NAO index is such that positive NAO years correspond to increases in $\Delta I^{\Delta physics}_{anthro_{\sigma 26.25-26.75}}$ (Table 1). This transfer of C_{anthro} from surface waters to the EDW through water mass transformation can sequester anthropogenic carbon for years to a few decades (the approximate residence time of interior water in the subtropical gyre [*Jenkins*, 1998; *Robbins and Jenkins*, 1998]). This consequently increases the magnitude of the subtropical C_{anthro} sink over these timescales. Changes in rates of mode water reventilation to the atmosphere may shorten or lengthen the timescale of C_{anthro} sequestration in the subtropical gyre [e.g., *Bates et al.*, 2002].

5. Mechanisms Governing Interannual Variability in the Subpolar Gyre

[31] In the model, variability in subsurface I_{anthro} in the subpolar gyre is primarily driven by changes along the

Table 1. The Relationship Between the Wintertime NAO Index and Changes in the Subtropical Mode Water (Eighteen Degree Water, EDW) and Subpolar Mode Water (SPMW) Outcrop Regions and Isopycnal Surfaces[a]

Relationship to NAO	Tg C or m: NAO Index Slope	Error	r Value	p Value
Subtropical EDW, 2 yr lag				
dI/dt (ΔPhysics) *	3.95	1.96	0.34	0.057
Outcrop mean MLD (ΔPhysics)	2.7	1.7	0.27	0.129
Outcrop CO2 flux (ΔPhysics)	0.2	0.12	0.28	0.115
Subpolar Mode Water, 0 yr lag				
dI/dt (ΔPhysics) **	3.1	1.0	0.48	0.0054
mean subpolar MLD (ΔPhysics)	7.57	1.65	0.63	5.0E-05
Outcrop CO2 flux (ΔPhysics)***	0.4	0.08	0.62	7.1E-05

[a]The slope is the slope for the best fit linear regression of the model output to the NAO index, the error is the error on the best fit slope, and the r and p values relate to the best fit slope. Ocean memory causes the subtropics to respond to NAO atmospheric forcing with a lag of 2 years. Therefore, the values for the subtropical EDW are given with this lag; *, σ26.5 between 15 and 40°N and 70–20°W > 150 m; **, σ27.675–27.7 between 45 and 66°N and 57–18°W; ***, σ27.6–27.7.

densest SPMW, $\sigma_{27.55–27.7}$. In the subpolar gyre, variability in the simulated mean winter MLD is significantly correlated with the NAO index such that the model mean winter MLD in the subpolar gyre is greater during positive NAO years than during negative NAO years (Figure 6a and Table 1). Deep winter mixed layers during positive NAO years correspond both to increased anthropogenic CO_2 flux into the subpolar gyre ($r = 0.71$, $p < 0.01$) and to increased ventilation of dense SPMW isopycnal surfaces (as defined by the intersection of the winter mixed layer with the isopycnal band). This results in a greater CO_2 flux onto the $\sigma_{27.5–27.7}$ isopycnal surfaces during positive NAO years as compared to negative NAO years (Figure 7). These findings are consistent with previous modeling studies which show that positive NAO years correlate with increased deep and intermediate water formation [*Lohmann et al.*, 2009] and increased air-sea CO_2 fluxes [*Thomas et al.*, 2008].

[32] The change in I_{anthro} for the $\sigma_{26.675–27.7}$ surface is compared to the anthropogenic air-sea CO_2 flux into the $\sigma_{27.6–27.7}$ outcrop region and the NAO index in Figure 6b. Here we use a larger outcrop region ($\sigma_{27.6–27.7}$) in order to account for local air-sea CO_2 flux into lighter isopycnals that are then transformed onto the $\sigma_{26.675–27.7}$ surface. The flux into $\sigma_{27.6–27.7}$ is positively correlated with $\Delta I_{anthro}^{\Delta physics}$ for $\sigma_{27.675–27.7}$ with a slope of 9.29 ± 2.5 $^{PgI_{anthro}a^{-1}}/_{PgCO_2a^{-1}}$ ($r = 0.55$, $p < 0.01$) for the regression of $\Delta I_{anthro}^{\Delta physics}$ on the wintertime air-sea CO_2 flux (smoothed with a three year running mean). This suggests that the local anthropogenic air-sea CO_2 flux only accounts for approximately 10% of the change in $\Delta I_{anthro}^{\Delta physics}$ (Figure 6b). Similarly, an analysis of the primary budget terms responsible for changes in $\Delta I_{anthro}^{\Delta physics}$ shows that only ~10% of changes in monthly $\Delta I_{anthro}^{\Delta physics}$ are due to gas exchange (see Text S1, section S4). As in the subtropics, the majority of monthly $\Delta I_{anthro}^{\Delta physics}$ variability is due to changes in advective DIC convergence. However, in the subpolar gyre, this relationship is driven by large changes in the horizontal advective carbon convergence that is compensated partially by similarly large, but inversely related, changes in the vertical advective carbon convergence. Part of this relationship may be explained by net mass convergence that is compensated by downwelling.

[33] Similar to the EDW, this analysis indicates that C_{anthro} storage in SPMW is primarily driven by water mass transformations rather than by local air-sea CO_2 gas exchange. This proposed mechanism for C_{anthro} storage is illustrated in Figure 5 using model output. Deep winter mixing homogenizes the upper water column redistributing the anthropogenic carbon, decreasing surface C_{anthro} and increasing C_{anthro} at depth (Figure 5d). The resulting increased C_{anthro} in the gyre interior persists after the mixing event (Figure 5f).

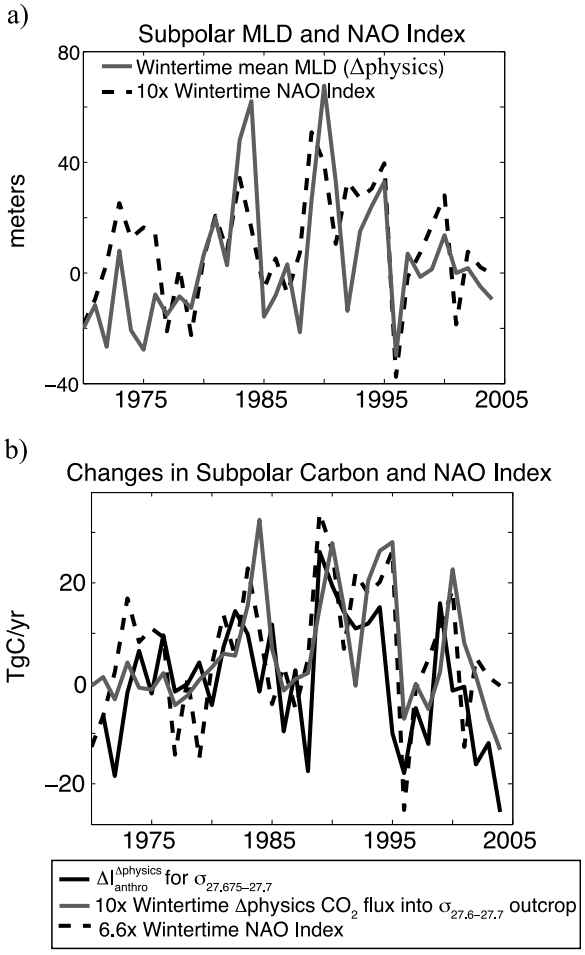

Figure 6. Impact of the NAO on model subpolar mixed layer depths and anthropogenic carbon fluxes. (a) The strong positive relationship between the impact of variable ocean physics on mean wintertime mixed layer depth (MLD(Δphysics)) for the subpolar gyre, 46°N–66°N 57°W–18°W, and the wintertime NAO index (scaled by a factor of 10). (b) The positive relationship between NAO index (scaled by a factor of 0.015), the impact of variable ocean physics on the change in anthropogenic carbon inventory ($\Delta I_{anthro}^{\Delta physics}$ in Tg C a^{-1}) for $\sigma_{27.675–27.7}$, and the impact of variable ocean physics on the anthropogenic air-sea CO_2 flux into the $\sigma_{27.6–27.7}$ wintertime outcrop (scaled by a factor of 10). The impact of variable ocean physics (Δphysics) is defined by equation (2).

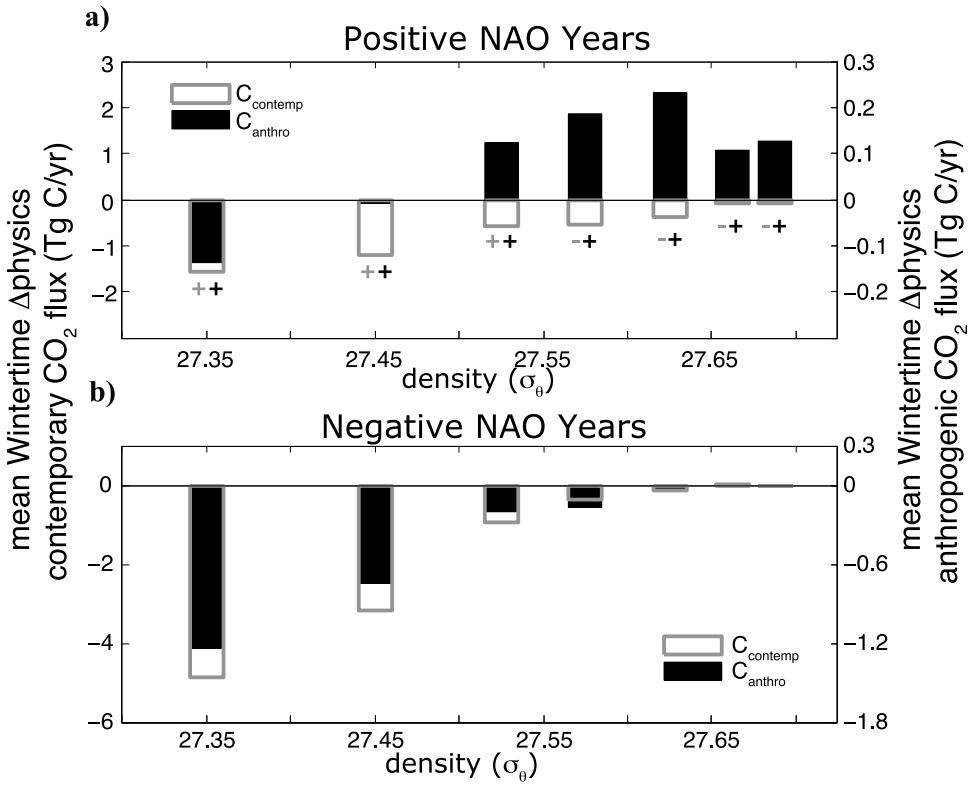

Figure 7. Wintertime anthropogenic and contemporary air-sea CO_2 flux onto Subpolar Mode Water isopycnal surfaces ($\sigma_{27.3-27.7}$). The impact of variable ocean physics (Δphysics) on the wintertime CO_2 flux onto seven isopycnal surfaces are shown for (a) positive and (b) negative NAO years, where Δphysics is defined by equation (2). The flux onto the isopycnal surfaces is defined as the total flux into model cells for which the wintertime mixed layer intersects with the wintertime depth of isopycnal band and is given in Pg C a^{-1}. Note the difference in scales for Figures 7a and 7b. The symbols in Figure 7a indicate an increase (+) or decrease (−) in the CO_2 flux during positive NAO years as compared to negative NAO years, where gray symbols represent contemporary carbon and black symbols represent anthropogenic carbon.

During the summer and early fall, anthropogenic carbon concentrations build back up in surface waters (Figures 5b and 5h), most likely due to advective transport of high anthropogenic CO_2 subtropical water, and the cycle repeats. Evidence for northward transport of high C_{anthro} surface waters is found both in hydrographic observations [e.g., *Álvarez et al.*, 2003, 2004; *Holfort et al.*, 1998; *Macdonald et al.*, 2003; *Omar and Olsen*, 2006; *Quay et al.*, 2007] and in numerical inversion studies [e.g., *Holfort et al.*, 1998; *Mikaloff Fletcher et al.*, 2006].

[34] Increased SPMW I_{anthro} translates into an increase in LSW I_{anthro}, which acts to sequester anthropogenic carbon on the timescale of years to several decades [*Haine et al.*, 2003; *Talley and McCartney*, 1982; *Waugh et al.*, 2004]. *Álvarez et al.* [2004] conclude that the net southward flow of the LSW is the largest contributor to the transport of C_{anthro} from the subpolar region into the subtropics. However, the long-term impact of increased SPMW I_{anthro} may be dampened by reventilation of SPMW C_{anthro}. Modeling work by *Haine et al.* [2003] suggests that 60% of waters subducted in the subpolar North Atlantic Ocean are reventilated to the atmosphere after 6–8 years.

[35] As discussed in section 3, variable ocean physics has a differential impact on SPMW anthropogenic and contemporary carbon concentrations. This is primarily due to differences in surface to depth concentration gradients between $C_{contemp}$ and C_{anthro} (Figure 5). During the winter, mixing acts to homogenize low $C_{contemp}$ surface waters with high $C_{contemp}$ subsurface waters thereby decreasing interior $C_{contemp}$ concentrations (Figures 5a and 5c), the opposite of what occurs to the anthropogenic carbon pool (Figures 5b and 5d). Winter mixing has a reduced impact on $C_{contemp}$ concentrations relative to the impact on C_{anthro} concentrations due to a substantially stronger surface to depth concentration gradient in C_{anthro}. The model also suggests that increased winter mixed layers during positive NAO years increases the efflux of natural carbon out of the densest SPMW surfaces (Figure 7).

6. Discussion: Implications for Observations

[36] In the model, we are able to easily separate anthropogenic and natural carbon. Therefore, in the above analysis, we are able to focus on the response of anthropogenic carbon uptake and storage to variable ocean physics. However, there is no simple way to differentiate between these two carbon pools in oceanographic observations. In general, observational estimates of anthropogenic carbon accumulation rates

rely on either the use of empirical methods (discussed in section 1) or on long-term monitoring of total carbon. The latter approach assumes a steady state ocean such that any long-term trends in total carbon or air-sea CO_2 flux can be attributed to anthropogenic carbon uptake. The accuracy of this approach can be improved by correcting for changes in salinity, dissolved oxygen, and nutrient concentrations. However, as discussed in section 3, there is not always a strong relationship between contemporary and anthropogenic carbon. The differential response of natural and anthropogenic carbon to variable ocean physics makes observations of changes in the ocean carbon sink substantially more difficult [e.g., *Lovenduski et al.*, 2008]. While we find good agreement between the observations and model predictions (sections 6.1 and 6.2), it is important to keep in mind that observational estimates of C_{anthro} may be impacted by changes in natural carbon that we have not addressed in the model analysis.

6.1. Subtropical Gyre

[37] The model simulations described above are consistent with the findings of *Bates et al.* [2002], *Gruber et al.* [2002] and *Bates* [2007] who report increased EDW DIC concentrations at the Bermuda Atlantic Time series Study site (BATS, 31°40′N, 64°10′W) during the late 1980s and 1990s. These authors attribute the increased EDW carbon sink to weakening wind speeds and reduced mixing events at BATS, which act to decrease ventilation of EDW C_{anthro} back to the atmosphere. Furthermore, *Gruber et al.* [2002] and *Bates* [2001] correlate the variability in winter MLD, sea surface temperature and DIC at BATS with shifts in the NAO phase. As discussed above, the southern extent of the simulated EDW outcrop oscillates between 33°N and 36°N in relation to the NAO phase such that the southern extent of the outcrop is closest to the BATS site during negative NAO years. *Bates et al.* [2002] find that EDW formation as far south as BATS decreases during positive NAO phases most likely due to weaker winter mixing. Similarly, in the model, annual mean MLDs and mean wintertime MLDs near Bermuda are lower for the period from 1988 to 2004 (positive NAO) as compared to 1970–1987 (neutral/negative NAO), though this difference is not statistically significant in the model output. Changes in the hydrographic properties at BATS reflect both the local response to climate variability and remote responses, such as changes in mode water formation rates, which are then advected laterally to BATS [*Jenkins*, 1982]. It is therefore difficult with observations alone to determine the mechanisms, local or remote, responsible for the interannual variability at BATS. However, the spatial and temporal resolution of the model, allows us to deconvolve these processes and propose an additional and potentially more important mechanism for the observed increase in the subtropical carbon sink during positive NAO years, e.g., 1988–1997. In the model, increased mixing and a larger EDW wintertime outcrop footprint during positive NAO years results in increased mode water formation. A thicker EDW isopycnal surface acts to sequester more anthropogenic carbon in the gyre interior. This results in increases in EDW C_{anthro} storage similar to that observed by *Bates et al.* [2002].

[38] An analysis of hydrographic data indicates large spatial and temporal variations in EDW renewal events with the outcrop region varying between 30°N–40°N [*Alfultis and Cornillon*, 2001], a similar range to that observed in the model. However, these authors do not suggest a mechanism for the observed variability in EDW renewal events. *Joyce et al.* [2000] find a high degree of correlation between positive NAO years, the northward extent of the Gulf Stream, and the thickness of the EDW (or potential vorticity of the EDW) near Bermuda. Similar to our findings, they conclude that the northward migration of the Gulf Stream in response to positive NAO forcing controls the formation of EDW in the Sargasso Sea.

6.2. Subpolar Gyre

[39] Two recent papers have evaluated changes in North Atlantic SPMW carbon inventories over the past several decades using a suite of hydrographic cruises. *Steinfeldt et al.* [2009] applied the transient tracer distribution method to hydrographic observations from 1997 and 2003 to estimate the impact of ocean variability on anthropogenic carbon inventories. These authors estimate that the change in physics between 1997 and 2003 resulted in a 6.4% decrease in northwestern Atlantic SPMW I_{anthro} ($27.1 \leq \sigma_\theta < 27.68$), a 64.8% increase in northwestern Atlantic upper LSW I_{anthro} ($27.68 \leq \sigma_\theta < 27.74$), and a 22% increase in dense SPMW I_{anthro} for the subpolar gyre ($27.68 \leq \sigma_\theta < 27.7$, 45°N–65°N, 57°W–18°W) (R. Steinfeldt, personal communication, 2010). The model shows a similar, though increased, response of a 17% decrease in northwestern Atlantic SPMW I_{anthro}, and a similar, though diminished, response of a 29.4% increase in northwestern Atlantic upper LSW I_{anthro}, and a 7.9% increase in subpolar $I_{anthro_{\sigma 27.675-27.7}}$ due to changing physics between 1997 and 2003. Both the observations and the model output show large differences in the response of different water masses to variable physics. Therefore, the apparent reduced impact of ocean physics on I_{anthro} in the model for upper LSW and $I_{anthro_{\sigma 27.675-27.7}}$ may be due to a slight offset in model mode water densities relative to the observed densities.

[40] *Pérez et al.* [2010] used the φC_T^o method to estimate C_{anthro} storage for different water masses in the northern North Atlantic. Following *Pérez et al.* 's definition of the Icelandic upper LSW, which most closely represents the dense SPMW focused on in this study ($\sigma_{0db} \geq 27.6$ and $\sigma_{1000db} < 32.3$, where 0 db and 1000 db are the reference pressures), we calculate a mean rate of increase from 1981 to 2004 of 0.40 ± 0.02 μmol kg^{-1} a^{-1} in the model. This matches well with the observed rate of increase reported by *Pérez et al.* of 0.40 + 0.06 μmol kg^{-1} a^{-1}. In addition, the model captures the observed decrease in accumulation rate in the late 1990s and early 2000s (1997–2005) as compared to the early 1990s (1992–1993); with an observed decrease in accumulation rate from 0.58 ± 0.82 μmol kg^{-1} a^{-1} to 0.39 ± 0.24 μmol kg^{-1} a^{-1} and a modeled decrease in accumulation rate from 0.64 ± 0.002 μmol kg^{-1}a^{-1} to 0.38 ± 0.01 μmol kg^{-1} a^{-1}. *Pérez et al.* suggest that the substantial decrease in accumulation rate during the second half of the 1990s may be due to changes in stratification and convection resulting from a shift in the NAO phase.

[41] The spatial and temporal resolution of the model provides additional insight into the mechanisms responsible for the observed changes in I_{anthro} and allows us to test the hypotheses proposed by the observations. As described above, the model output indicates that the observed decrease in C_{anthro} uptake and storage during negative NAO years

results from decreased mixed layer depths and dense SPMW water mass transformation which act to decrease the transfer of high C_{anthro} surface waters into the ocean interior. In addition, our results suggest that the majority of subsurface I_{anthro} is derived from surface waters advected into the region with only ~10% derived from local air-sea CO_2 flux. Finally, this and other recent work [*Schuster et al.*, 2009; *Thomas et al.*, 2008] highlight the importance of understanding interannual variability in the interpretation of hydrographic observations in which may alias decadal variability into estimates of long-term trends.

7. Conclusions

[42] Interannual variability impacts the anthropogenic carbon inventory of the North Atlantic Ocean. In both the subtropical and subpolar gyres, increased anthropogenic carbon (C_{anthro}) uptake occurs as a result of increased mode water formation and air-sea CO_2 exchange during the winter months. Changes in the frequency, duration and intensity of mode water formation events are related to shifts in winds, circulation patterns and winter storms associated in part with shifts in the North Atlantic Oscillation. In our 'Variable Physics' model simulations, positive NAO years correspond with increased anthropogenic carbon inventories ($\Delta I_{anthro}^{\Delta physics}$) in both the subpolar and subtropical gyres relative to the 'Repeat Annual Cycle' simulations. In both gyres, changes in local anthropogenic air-sea CO_2 flux into mode waters account for only ~10% of changes in mode water $I_{anthro}^{\Delta physics}$. We conclude that mode water $I_{anthro}^{\Delta physics}$ is primarily driven by water mass transformation in which light, high C_{anthro}, surface waters are entrained onto deeper isopycnal surfaces through diapycnal mixing and surface buoyancy heat flux. This implies that much of the anthropogenic carbon found in the ocean interior is derived from surface waters advected into the water formation region rather than from local gas exchange. Our findings also suggest that climate modes, such as the NAO, can alter the residence time of anthropogenic carbon in the ocean by altering the rate of water mass transformation that act to transport surface C_{anthro} into the ocean thermocline, where it is sequestered for several years to several decades. In addition, increased frequency of positive NAO years, such as is predicted by climate models [*Meehl et al.*, 2007], could increase the strength of the North Atlantic Ocean sink by increasing mode water formation. However, these changes may be reduced due to other climate feedbacks such as an increased freshwater flux in the Labrador and Nordic seas that may act to decrease deep water formation [e.g., *Thorpe et al.*, 2001], or increased stratification in the subtropics resulting from secular increases in surface temperatures [e.g., *Boyd and Doney*, 2002; *Intergovernmental Panel on Climate Change*, 2001].

[43] Observations are easily biased by sampling strategy and the time period of observations. In addition, it is difficult to parcel out observed inventory changes that are due to lateral sloshing and vertical heave from those resulting in varied uptake rates. *Rodgers et al.* [2009] suggest that altimetry data in conjunction with numerical models may help correct for some of the interannual variability in observed DIC concentrations. Similarly, we conclude that numerical models can aid in providing both a context for hydrographic observations and an understanding of the driving mechanisms behind observed trends.

[44] **Acknowledgments.** We would like to acknowledge funding from the NOAA Climate Program under the Office of Climate Observations and Global Carbon Cycle Program (NOAA-NA07OAR4310098), NSF (OCE-0623034), NCAR, the WHOI Ocean Climate Institute, a National Defense Science and Engineering Graduate Fellowship and an Environmental Protection Agency STAR graduate fellowship. NCAR is sponsored by the National Science Foundation. We would like to thank R. Steinfeldt for providing observed anthropogenic carbon inventories for the Subpolar Mode Waters. We would also like to acknowledge the helpful comments of anonymous reviewers.

References

Alfultis, M. A., and P. Cornillon (2001), Annual and interannual changes in the North Atlantic STMW layer properties, *J. Phys. Oceanogr.*, *31*(8), 2066–2086, doi:10.1175/1520-0485(2001)031<2066:AAICIT>2.0.CO;2.

Álvarez, M., et al. (2003), Transports and budgets of total inorganic carbon in the subpolar and temperate North Atlantic, *Global Biogeochem. Cycles*, *17*(1), 1002, doi:10.1029/2002GB001881.

Álvarez, M., et al. (2004), Physical and biogeochemical transports structure in the North Atlantic subpolar gyre, *J. Geophys. Res.*, *109*, C03027, doi:10.1029/2003JC002015.

Bates, N. R. (2001), Interannual variability of oceanic CO_2 and biogeochemical properties in the Western North Atlantic subtropical gyre, *Deep Sea Res., Part II*, *48*(8–9), 1507–1528, doi:10.1016/S0967-0645(00)00151-X.

Bates, N. R. (2007), Interannual variability of the oceanic CO_2 sink in the subtropical gyre of the North Atlantic Ocean over the last 2 decades, *J. Geophys. Res.*, *112*, C09013, doi:10.1029/2006JC003759.

Bates, N. R., et al. (2002), A short-term sink for atmospheric CO_2 in subtropical mode water of the North Atlantic Ocean, *Nature*, *420*(6915), 489–493.

Boyd, P. W., and S. C. Doney (2002), Modeling regional responses by marine pelagic ecosystems to global climate change, *Geophys. Res. Lett.*, *29*(16), 1806, doi:10.1029/2001GL014130.

Brambilla, E., and L. D. Talley (2008), Subpolar Mode Water in the northeastern Atlantic: 1. Averaged properties and mean circulation, *J. Geophys. Res.*, *113*, C04025, doi:10.1029/2006JC004062.

Brambilla, E., et al. (2008), Subpolar Mode Water in the northeastern Atlantic: 2. Origin and transformation, *J. Geophys. Res.*, *113*, C04026, doi:10.1029/2006JC004063.

Brewer, P. G., et al. (1995), The pH of the North Atlantic Ocean: Improvements to the global model for sound absorption in seawater, *J. Geophys. Res.*, *100*(C5), 8761–8776, doi:10.1029/95JC00306.

Canadell, J. G., et al. (2007), Contributions to accelerating atmospheric CO_2 growth from economic activity, carbon intensity, and efficiency of natural sinks, *Proc. Natl. Acad. Sci. U. S. A.*, *104*(47), 18,866–18,870, doi:10.1073/pnas.0702737104.

Corbière, A., et al. (2007), Interannual and decadal variability of the oceanic carbon sink in the North Atlantic subpolar gyre, *Tellus, Ser. B*, *59*(2), 168–178, doi:10.1111/j.1600-0889.2006.00232.x.

Curry, R. G., and M. S. McCartney (2001), Ocean gyre circulation changes associated with the North Atlantic Oscillation, *J. Phys. Oceanogr.*, *31*(12), 3374–3400, doi:10.1175/1520-0485(2001)031<3374:OGCCAW>2.0.CO;2.

Doney, S. C., et al. (2006), Natural variability in a stable, 1000 yr global coupled climate–carbon cycle simulation, *J. Clim.*, *19*(13), 3033–3054, doi:10.1175/JCLI3783.1.

Doney, S. C., et al. (2007), Mechanisms governing interannual variability of upper ocean temperature in a global ocean hindcast simulation, *J. Phys. Oceanogr.*, *37*(7), 1918–1938, doi:10.1175/JPO3089.1.

Doney, S. C., et al. (2009a), Mechanisms governing interannual variability in upper ocean inorganic carbon system and air-sea CO_2 fluxes: Physical climate and atmospheric dust, *Deep Sea Res., Part II*, *56*(8–10), 640–655, doi:10.1016/j.dsr2.2008.12.006.

Doney, S. C., et al. (2009b), Skill metrics for confronting global upper ocean ecosystem-biogeochemistry models against field and remote sensing data, *J. Mar. Syst.*, *76*(1–2), 95–112, doi:10.1016/j.jmarsys.2008.05.015.

Friedlingstein, P., et al. (2006), Climate–carbon cycle feedback analysis: Results from the C^4MIP model intercomparison, *J. Clim.*, *19*(14), 3337–3353, doi:10.1175/JCLI3800.1.

Friis, K., et al. (2005), On the temporal increase of anthropogenic CO_2 in the subpolar North Atlantic, *Deep Sea Res., Part I*, *52*(5), 681–698, doi:10.1016/j.dsr.2004.11.017.

Fung, I. Y., et al. (2005), Evolution of carbon sinks in a changing climate, *Proc. Natl. Acad. Sci. U. S. A.*, *102*(32), 11,201–11,206, doi:10.1073/pnas.0504949102.

Gent, P. R., and J. C. McWilliams (1990), Isopycnal Mixing in Ocean Circulation Models, *J. Phys. Oceanogr.*, *20*(1), 150–155, doi:10.1175/1520-0485(1990)020<0150:IMIOCM>2.0.CO;2.

Gruber, N., et al. (1996), An improved method for detecting anthropogenic CO_2 in the oceans, *Global Biogeochem. Cycles*, *10*(4), 809–837, doi:10.1029/96GB01608.

Gruber, N., et al. (2002), Interannual variability in the North Atlantic Ocean carbon sink, *Science*, *298*(5602), 2374–2378, doi:10.1126/science.1077077.

Haine, T. W. N., et al. (2003), Chlorofluorocarbon constraints on North Atlantic ventilation, *J. Phys. Oceanogr.*, *33*(8), 1798–1814, doi:10.1175/1520-0485(2003)033<1798:CCONAV>2.0.CO;2.

Holfort, J., et al. (1998), Meridional transport of dissolved inorganic carbon in the South Atlantic Ocean, *Global Biogeochem. Cycles*, *12*(3), 479–499, doi:10.1029/98GB01533.

Hurrell, J. W. (1995), Decadal trends in the North Atlantic Oscillation: Regional temperatures and precipitation, *Science*, *269*(5224), 676–679, doi:10.1126/science.269.5224.676.

Hurrell, J. W., and C. Deser (2009), North Atlantic climate variability: The role of the North Atlantic Oscillation, *J. Mar. Syst.*, *78*(1), 28–41, doi:10.1016/j.jmarsys.2008.11.026.

Hurrell, J. W., et al. (2001), Climate: The North Atlantic Oscillation, *Science*, *291*(5504), 603–605, doi:10.1126/science.1058761.

Hurrell, J. W., Y. Kushnir, G. Ottersen, and M. Visbeck (Eds.) (2003), *An Overview of the North Atlantic Oscillation: Climatic Significance and Environmental Impact*, *Geophys. Monograph Ser.*, vol. 134, 35 pp., AGU, Washington, D. C.

Intergovernmental Panel on Climate Change (2001), Climate Change 2001: The Scientific Basis. Contribution of Working Group I to the Third Assessment Report of the Intergovernmental Panel on Climate Change, 881 pp., Cambridge Univ. Press, Cambridge, U. K.

Jenkins, W. J. (1982), On the climate of a subtropical ocean gyre: Decade timescale variations in water mass renewal in the Sargasso Sea, *J. Mar. Res.*, *40*, 265–290.

Jenkins, W. J. (1998), Studying subtropical thermocline ventilation and circulation using tritium and He 3, *J. Geophys. Res.*, *103*(C8), 15,817–15,831, doi:10.1029/98JC00141.

Joyce, T. M., et al. (2000), The relation between decadal variability of subtropical mode water and the North Atlantic Oscillation, *J. Clim.*, *13*(14), 2550–2569, doi:10.1175/1520-0442(2000)013<2550:TRBDVO>2.0.CO;2.

Keeling, C. D., and T. P. Whorf (1994), Atmospheric CO_2 records from sites in the SIO air sampling network, in *Trends '93: A Compendium of Data on Global Change*, edited by T. A. Boden et al., pp. 16–26, ORNL/CDIAC-65, Carbon Dioxide Inf. Anal. Cent., Oak Ridge Natl. Lab., Oak Ridge, Tenn.

Keeling, C. D., et al. (1976), Atmospheric carbon dioxide variations at Mauna Loa Observatory, Hawaii, *Tellus*, *28*(6), 538–551, doi:10.1111/j.2153-3490.1976.tb00701.x.

Key, R. M., et al. (2004), A global ocean carbon climatology: Results from Global Data Analysis Project (GLODAP), *Global Biogeochem. Cycles*, *18*, GB4031, doi:10.1029/2004GB002247.

Khatiwala, S., et al. (2009), Reconstruction of the history of anthropogenic CO_2 concentrations in the ocean, *Nature*, *462*(7271), 346–349, doi:10.1038/nature08526.

Large, W. G., and S. G. Yeager (2004), Diurnal to decadal global forcing for ocean and sea-ice models: The data sets and flux climatologies, *NCAR Tech. Note NCAR/TN-460+STR*, Natl. Cent. for Atmos. Res., Boulder, Colo.

Lee, K., et al. (2003), An updated anthropogenic CO_2 inventory in the Atlantic ocean, *Global Biogeochem. Cycles*, *17*(4), 1116, doi:10.1029/2003GB002067.

Lefèvre, N., et al. (2004), A decrease in the sink for atmospheric CO_2 in the North Atlantic, *Geophys. Res. Lett.*, *31*, L07306, doi:10.1029/2003GL018957.

Le Quéré, C., et al. (2009), Trends in the sources and sinks of carbon dioxide, *Nat. Geosci.*, *2*(12), 831–836, doi:10.1038/ngeo689.

Le Quéré, C., et al. (2010), Impact of climate change and variability on the global oceanic sink of CO_2, *Global Biogeochem. Cycles*, *24*, GB4007, doi:10.1029/2009GB003599.

Levine, N. M., et al. (2008), Impact of ocean carbon system variability on the detection of temporal increases in anthropogenic CO_2, *J. Geophys. Res.*, *113*, C03019, doi:10.1029/2007JC004153.

Lohmann, K., et al. (2009), Response of the North Atlantic subpolar gyre to persistent North Atlantic oscillation like forcing, *Clim. Dyn.*, *32*(2–3), 273–285, doi:10.1007/s00382-008-0467-6.

Lovenduski, N. S., et al. (2008), Toward a mechanistic understanding of the decadal trends in the Southern Ocean carbon sink, *Global Biogeochem. Cycles*, *22*, GB3016, doi:10.1029/2007GB003139.

Macdonald, A. M., et al. (2003), A 1998–1992 comparison of inorganic carbon and its transport across 24.5°N in the Atlantic, *Deep Sea Res. Part II*, *50*(22–26), 3041–3064.

Mariano, A. J., E. H. Ryan, B. D. Perkins, and S. Smithers (1995), *The Mariano Global Surface Velocity Analysis 1.0*, *U. S. Coast Guard Tech. Rep. CG-D-34-95*, Natl. Tech. Inf. Serv., Springfield, Va.

Marshall, J., et al. (2001), North Atlantic climate variability: Phenomena, impacts and mechanisms, *Int. J. Climatol.*, *21*(15), 1863–1898, doi:10.1002/joc.693.

Marshall, J., et al. (2009), The CLIMODE field campaign: Observing the cycle of convection and restratification over the Gulf Stream, *Bull. Am. Meteorol. Soc.*, *90*(9), 1337–1350.

Marshall, J. C., et al. (1993), Inferring the subduction rate and period over the North Atlantic, *J. Phys. Oceanogr.*, *23*(7), 1315–1329, doi:10.1175/1520-0485(1993)023<1315:ITSRAP>2.0.CO;2.

Matsumoto, K., and N. Gruber (2005), How accurate is the estimation of anthropogenic carbon in the ocean? An evaluation of the ΔC^* method, *Global Biogeochem. Cycles*, *19*, GB3014, doi:10.1029/2004GB002397.

McCartney, M. S., and L. D. Talley (1982), The sub-polar mode water of the North Atlantic ocean, *J. Phys. Oceanogr.*, *12*(11), 1169–1188, doi:10.1175/1520-0485(1982)012<1169:TSMWOT>2.0.CO;2.

McKinley, G. A., et al. (2004), Mechanisms of air-sea CO_2 flux variability in the equatorial Pacific and the North Atlantic, *Global Biogeochem. Cycles*, *18*, GB2011, doi:10.1029/2003GB002179.

Meehl, G. A., et al. (2007), Global climate projections, in *Climate Change 2007: The Physical Scince Basis. Contribution of Working Group I to the Fourth Assessment Report of the Intergovernmental Panel on Climate Change*, edited by S. Solomon et al., pp. 747–845, Cambridge Univ. Press, Cambridge, U. K.

Mikaloff Fletcher, S. E., et al. (2006), Inverse estimates of anthropogenic CO_2 uptake, transport, and storage by the ocean, *Global Biogeochem. Cycles*, *20*, GB2002, doi:10.1029/2005GB002530.

Moore, J. K., et al. (2004), Upper ocean ecosystem dynamics and iron cycling in a global three-dimensional model, *Global Biogeochem. Cycles*, *18*, GB4028, doi:10.1029/2004GB002220.

Olsen, A., et al. (2006), Magnitude and origin of the anthropogenic CO_2 increase and ^{13}C Suess effect in the Nordic seas since 1981, *Global Biogeochem. Cycles*, *20*, GB3027, doi:10.1029/2005GB002669.

Omar, A. M., and A. Olsen (2006), Reconstructing the time history of the air-sea CO2 disequilibrium and its rate of change in the eastern subpolar North Atlantic, 1972–1989, *Geophys. Res. Lett.*, *33*, L04602, doi:10.1029/2005GL025425.

Pérez, F. F., et al. (2008), Temporal variability of the anthropogenic CO_2 storage in the Irminger Sea, *Biogeosciences*, *5*(6), 1669–1679, doi:10.5194/bg-5-1669-2008.

Pérez, F. F., et al. (2010), Trends of anthropogenic CO_2 storage in North Atlantic water masses, *Biogeosciences*, *7*(5), 1789–1807, doi:10.5194/bg-7-1789-2010.

Quay, P., et al. (2007), Anthropogenic CO_2 accumulation rates in the North Atlantic Ocean from changes in the $^{13}C/^{12}C$ of dissolved inorganic carbon, *Global Biogeochem. Cycles*, *21*, GB1009, doi:10.1029/2006GB002761.

Robbins, P. E., and W. J. Jenkins (1998), Observations of temporal changes of tritium-He-3 age in the eastern North Atlantic thermocline: Evidence for changes in ventilation?, *J. Mar. Res.*, *56*(5), 1125–1161, doi:10.1357/002224098765173482.

Rodgers, K. B., et al. (2009), Using altimetry to help explain patchy changes in hydrographic carbon measurements, *J. Geophys. Res.*, *114*, C09013, doi:10.1029/2008JC005183.

Rogers, J. C. (1984), The association between the North Atlantic Oscillation and the Southern Oscillation in the Northern Hemisphere, *Mon. Weather Rev.*, *112*(10), 1999–2015, doi:10.1175/1520-0493(1984)112<1999:TABTNA>2.0.CO;2.

Sabine, C. L., and T. Tanhua (2010), Estimation of anthropogenic CO_2 inventories in the ocean, *Annu. Rev. Mar. Sci.*, *2*, 175–198, doi:10.1146/annurev-marine-120308-080947.

Sabine, C. L., et al. (2004), The oceanic sink for anthropogenic CO_2, *Science*, *305*(5682), 367–371, doi:10.1126/science.1097403.

Sarmiento, J. L., et al. (1995), Air-sea CO_2 transfer and the carbon budget of the North Atlantic, *Philos. Trans. R. Soc. London, Ser. B*, *348*(1324), 211–219, doi:10.1098/rstb.1995.0063.

Schuster, U., and A. J. Watson (2007), A variable and decreasing sink for atmospheric CO_2 in the North Atlantic, *J. Geophys. Res.*, *112*, C11006, doi:10.1029/2006JC003941.

Schuster, U., et al. (2009), Trends in North Atlantic sea-surface fCO(2) from 1990 to 2006, *Deep Sea Res., Part II*, *56*(8–10), 620–629, doi:10.1016/j.dsr2.2008.12.011.

Steinfeldt, R., et al. (2009), Inventory changes in anthropogenic carbon from 1997–2003 in the Atlantic Ocean between 20°S and 65°N, *Global Biogeochem. Cycles*, *23*, GB3010, doi:10.1029/2008GB003311.

Takahashi, T., et al. (2009), Climatological mean and decadal change in surface ocean pCO_2, and net sea-air $_{CO2}$ flux over the global oceans, *Deep Sea Res., Part II*, *56*(8–10), 554–577, doi:10.1016/j.dsr2.2008.12.009.

Talley, L., and M. Raymer (1982), Eighteen Degree Water variability, *J. Mar. Res.*, *40*, suppl., 757–775.

Talley, L. D., and M. S. McCartney (1982), Distribution and circulation of Labrador Sea Water, *J. Phys. Oceanogr.*, *12*(11), 1189–1205, doi:10.1175/1520-0485(1982)012<1189:DACOLS>2.0.CO;2.

Thomas, H., et al. (2008), Changes in the North Atlantic Oscillation influence CO_2 uptake in the North Atlantic over the past 2 decades, *Global Biogeochem. Cycles*, *22*, GB4027, doi:10.1029/2007GB003167.

Thorpe, R. B., et al. (2001), Mechanisms determining the Atlantic thermohaline circulation response to greenhouse gas forcing in a non-flux-adjusted coupled climate model, *J. Clim.*, *14*(14), 3102–3116, doi:10.1175/1520-0442(2001)014<3102:MDTATC>2.0.CO;2.

Touratier, F., and C. Goyet (2004), Definition, properties, and Atlantic Ocean distribution of the new tracer TrOCA, *J. Mar. Syst.*, *46*(1–4), 169–179, doi:10.1016/j.jmarsys.2003.11.016.

Ullman, D. J., et al. (2009), Trends in the North Atlantic carbon sink: 1992–2006, *Global Biogeochem. Cycles*, *23*, GB4011, doi:10.1029/2008GB003383.

Vázquez-Rodríguez, M., et al. (2009), Anthropogenic carbon distributions in the Atlantic Ocean: Data-based estimates from the Arctic to the Antarctic, *Biogeosciences*, *6*(3), 439–451, doi:10.5194/bg-6-439-2009.

Visbeck, M., et al. (Eds.) (2003), The ocean's response to North Atlantic Oscillation variability, in *The North Atlantic Oscillation: Climatic Significance and Environmental Impact*, *Geophys. Monograph Ser.*, vol. 134, edited by J. W. Hurrell et al., pp. 113–146, AGU, Washington, D. C.

Wallace, D. (1995), *Monitoring Global Ocean Carbon Inventories*, 54 pp., Ocean Observing Syst. Dev. Panel, Texas A&M Univ., College Station, Tex.

Wallace, D. (2001), Storage and transport of excess CO_2 in the ocean: The JGOFS/WOCE global CO_2 survey, in *Ocean Circulation and Climate*, edited by G. Siedler et al., pp. 489–521, Academic, San Diego, Calif., doi:10.1016/S0074-6142(01)80136-4.

Wanninkhof, R., et al. (2010), Detecting anthropogenic CO_2 changes in the interior Atlantic Ocean between 1989–2005, *J. Geophys. Res.*, *115*, C11028, doi:10.1029/2010JC006251.

Watson, A. J., et al. (2009), Tracking the variable North Atlantic sink for atmospheric CO_2, *Science*, *326*(5958), 1391–1393, doi:10.1126/science.1177394.

Waugh, D. W., et al. (2004), Transport times and anthropogenic carbon in the subpolar North Atlantic Ocean, *Deep Sea Res., Part I*, *51*(11), 1475–1491.

Waugh, D. W., et al. (2006), Anthropogenic CO_2 in the oceans estimated using transit time distributions, *Tellus, Ser. B*, *58*(5), 376–389, doi:10.1111/j.1600-0889.2006.00222.x.

N. R. Bates, Bermuda Institute of Ocean Sciences, St. George's, GE 01, Bermuda.

S. C. Doney and I. Lima, Marine Chemistry and Geochemistry, Woods Hole Oceanographic Institution, Woods Hole, MA 02543, USA.

R. A. Feely, NOAA/PMEL, Seattle, WA 98115, USA.

N. M. Levine, Department of Organismic and Evolutionary Biology, Harvard University, Cambridge, MA 02138, USA. (nlevine@oeb.harvard.edu)

R. Wanninkhof, NOAA/AOML, Miami, FL 33149, USA.